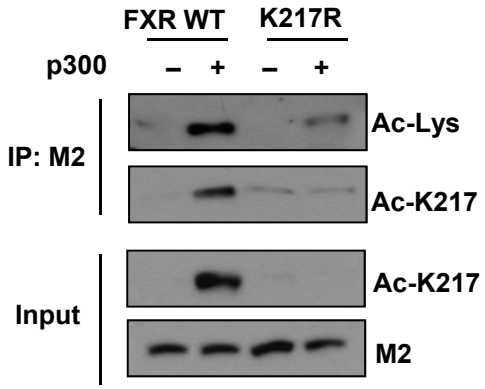


**Figure S1. Quality and specificity of an Ac-K217 FXR antibody.**
Cos-1 cells were cotransfected with the expression plasmids 3flag-FXR-WT or K217R along with p300. Cells were treated with 200 nM of GW4064 and deacetylase inhibitors (500 nM trichostain A and 10 mM nicotinamide) for 2 to 5 h before harvesting. Flag-FXR was bound to M2 agarose and acetylation of FXR was detected by IB using pan acetyl lysine antibody (Ac-lys) or Ac-K217 FXR antibody (Ac-K217). Flag-FXR levels and Ac-K217 FXR levels in input sample were also detected by IB.

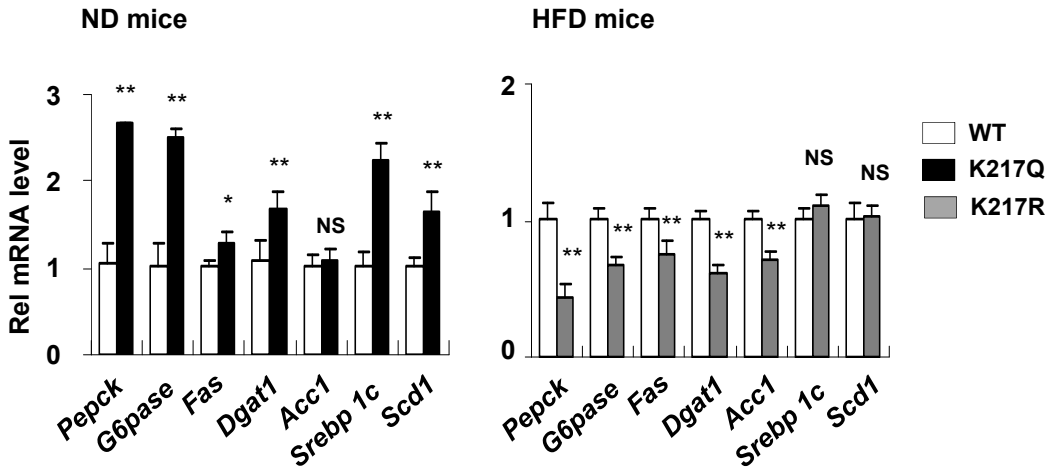


**Figure S2. Effects of acetylation of FXR at K217 on expression of gluconeogenic and lipogenic genes in mouse liver.**
FXR-WT or K217 mutants were adenovirally expressed in livers of lean or HFD obese mice and the mRNA levels of indicated genes were measured by q-RTPCR (n=4,*p<0.05, **p<0.005, NS, not significant).

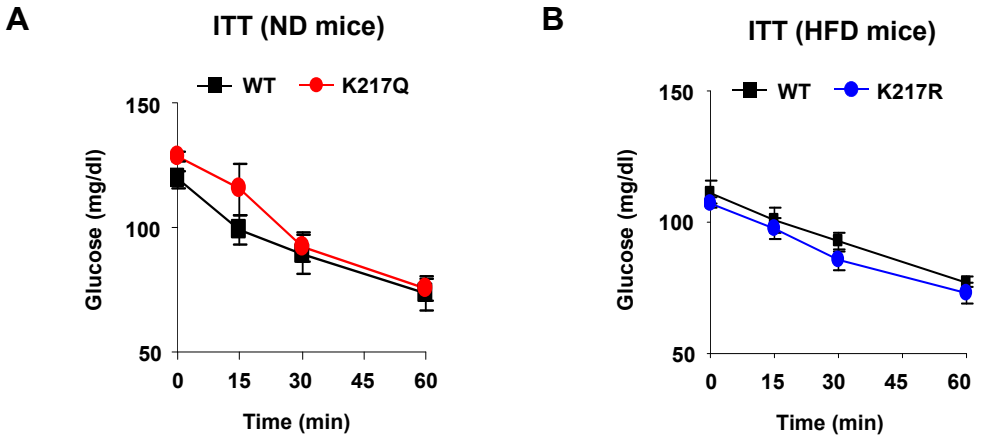


**Figure S3. Effects of acetylation of FXR at K217 on insulin resistance.**
FXR-WT or K217 mutants were adenovirally expressed in livers of lean (ND) (A) or obese (HFD) (B) mice as indicated. For the insulin tolerance test (ITT), serum glucose levels were measured at the indicated times after i.p. injection of insulin (n=4 mice).

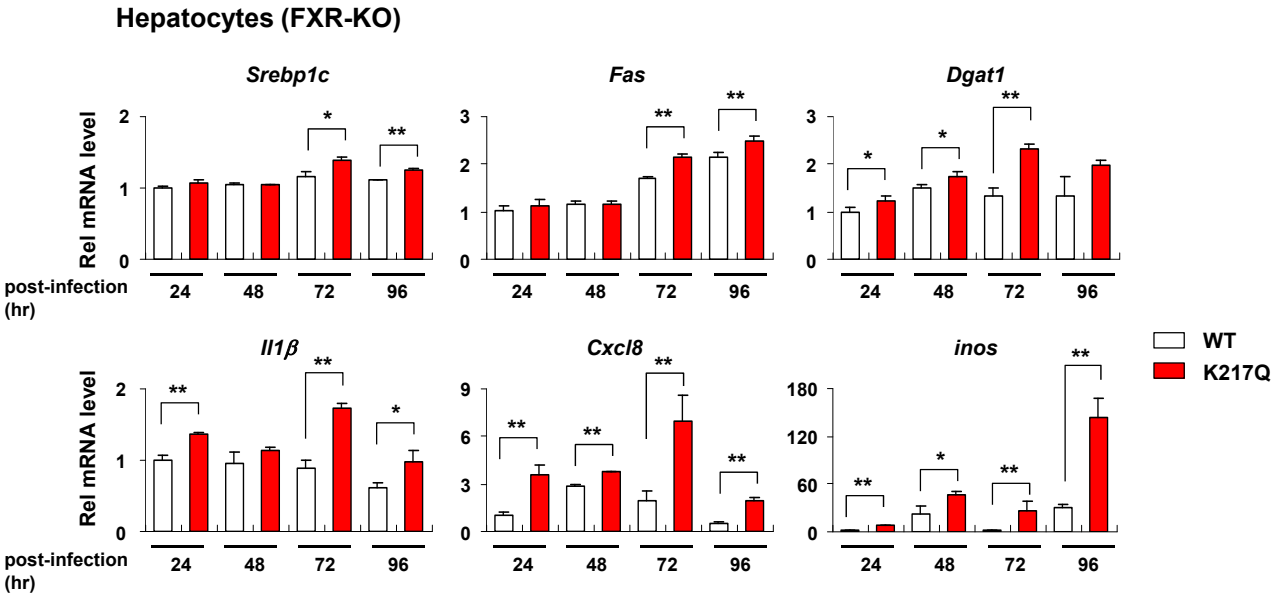


**Figure S4. Effects of acetylation of FXR at K217 on expression of lipogenic and inflammatory genes in hepatocytes.**

Hepatocytes were isolated from FXR-KO mice infected with an adenoviral vector expressing FXR-WT or the K217Q mutant and then, mRNA levels of lipogenic and proinflammatory genes as a function of time after adenoviral infection were detected by q-RTRPCR.

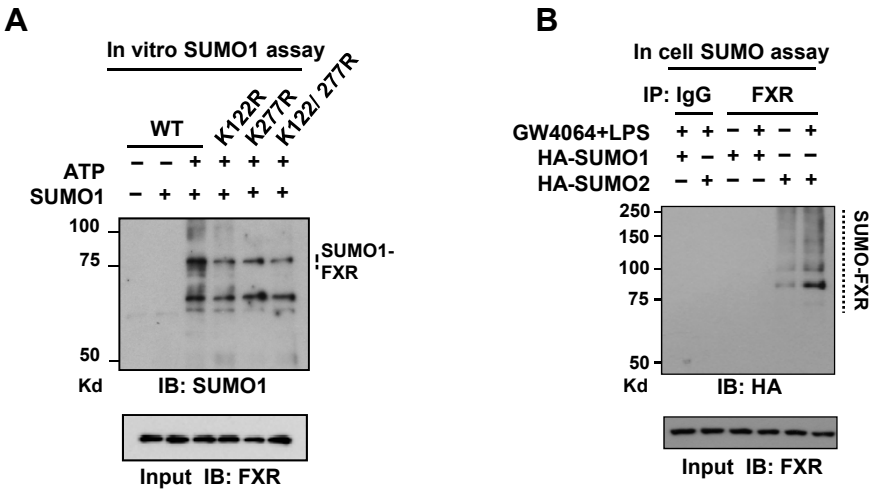


**Figure S5. FXR is SUMO1-modified at multiple lysines in vitro, but SUMO1-FXR is not detected, whereas SUMO2-FXR levels are increased, after treatment with LPS and GW4064 in cells.**

(A) In vitro SUMO assay: Flag-FXR-WT or FXR mutants (K122R, K277R, or K122/277R) were adenovirally expressed in Cos-1 cells that were then treated with GW4064 and isolated by binding to M2 agarose. Then, in vitro SUMO assays were performed by incubation of purified flag-FXR WT or mutant with purified SUMO components, including SUMO1 protein. Unincorporated SUMO components were removed by washing and SUMO1 modification of FXR was detected by IB. (B) In cell SUMO assay: Cos-1 cells were transfected with expression plasmids for flag-FXR WT, and either HA-SUMO1 or HA-SUMO2 and 48h later, cells were treated with GW4064 and LPS as indicated and SUMO1-FXR or SUMO2-FXR levels were detected by IP/IB.

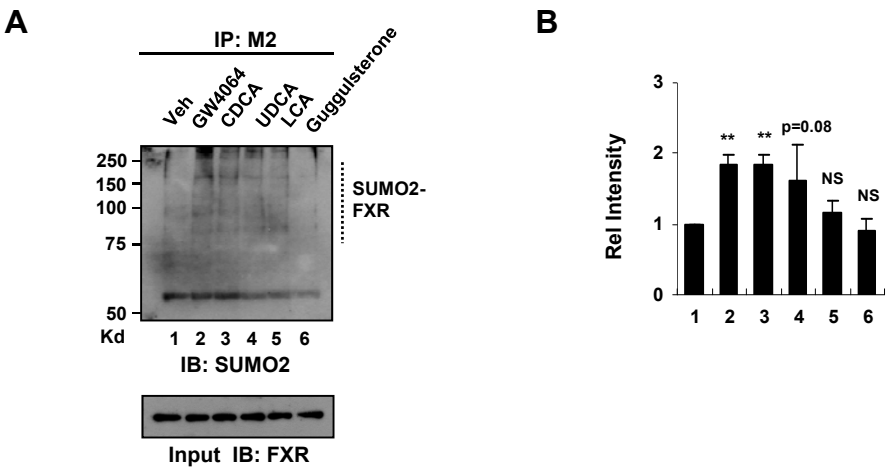


**Figure S6. Effects of treatment with synthetic or natural FXR ligands on SUMO2 modification in hepatocytes.**

(A) Primary mouse hepatocytes were infected with an adenoviral vector expressing f-FXR-WT and then, treated with each of FXR ligands as indicated, and SUMO2-FXR levels were measured by IP/IB. FXR levels in input samples are shown below. (B) SUMO assays in hepatocytes were repeated three times and relative SUMO2-FXR levels were quantified (n=3, **p<0.005).

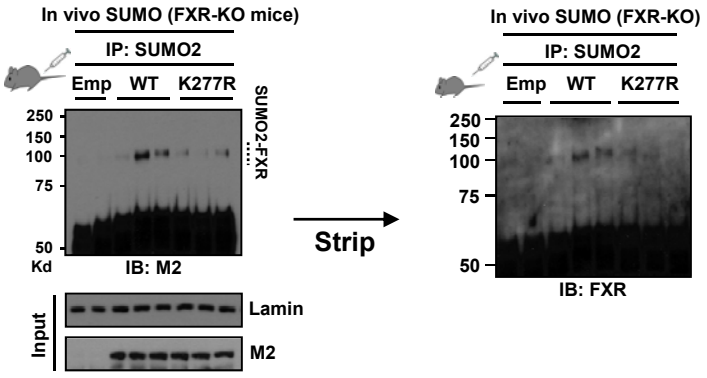


**Figure S7. Effects of K277R mutation in FXR on SUMO2 modification in mouse liver.**

In vivo SUMO assays were performed as described in experimental procedures. After SUMO2-flag-FXR levels were detected by IB (left panel) and then, the membrane was stripped and FXR was detected by IB using FXR antibody (right panel).

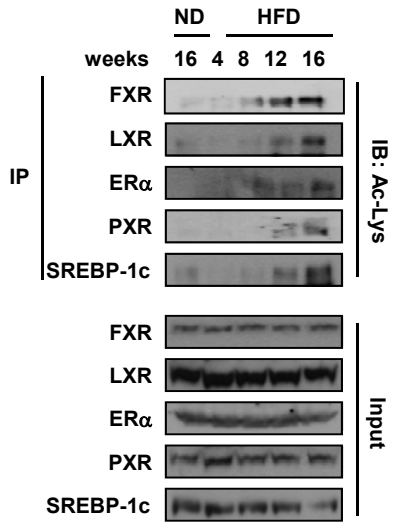


**Figure S8. Effects of feeding a HFD for different times on acetylation of transcriptional regulators in mouse liver.**
Livers from 3 mice fed a HFD for the indicated times were pooled, liver extracts were prepared, and the acetylated transcriptional regulator levels were detected by IP/IB. Hepatic expression of transcriptional regulators detected by IB are shown below.

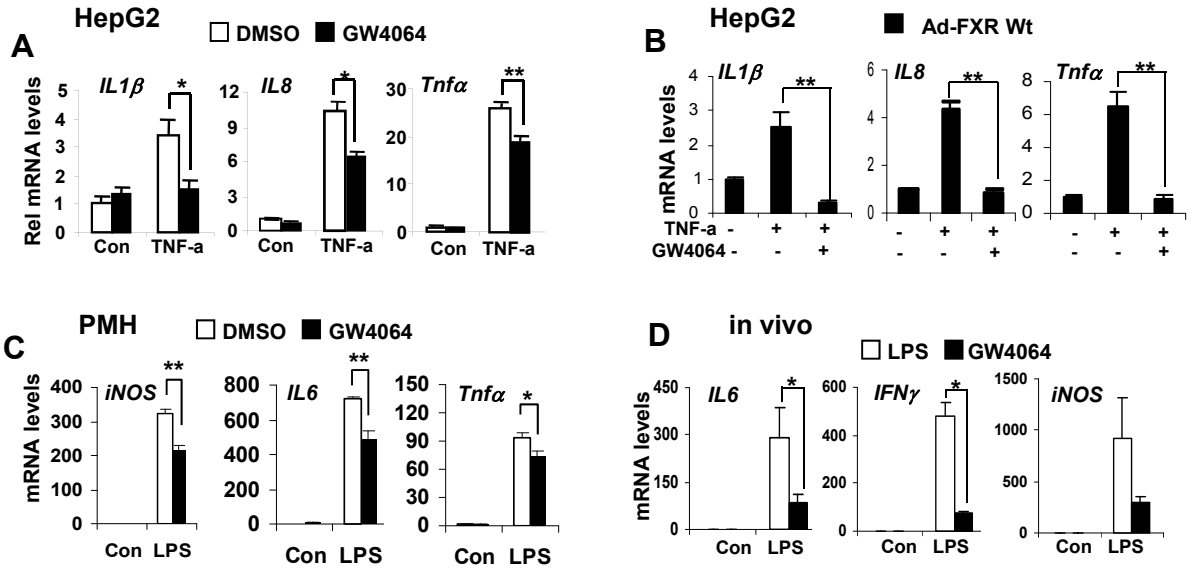


**Figure S9. Effects of activation of FXR signaling on expression of inflammatory genes in hepatic cells, hepatocytes, and mouse liver in vivo.**

**(**A) HepG2 cells were treated with GW4064, and mRNA levels of indicated genes were measured by q-RTPCR. (B) HepG2 cells were infected with an adenoviral vector expressing FXR-WT and then treated with TNFa and/or GW4064 as indicated, and q-RTRPCR was performed. (C) Hepatocytes were isolated from mice and treated with LPS and/or GW4064 as indicated, and q-RTPCR was performed. (D) Mice were treated with LPS and/or GW4064 as indicated, and q-RTPCR was performed. (SEM, n=4, *p<0.05, **p<0.005).

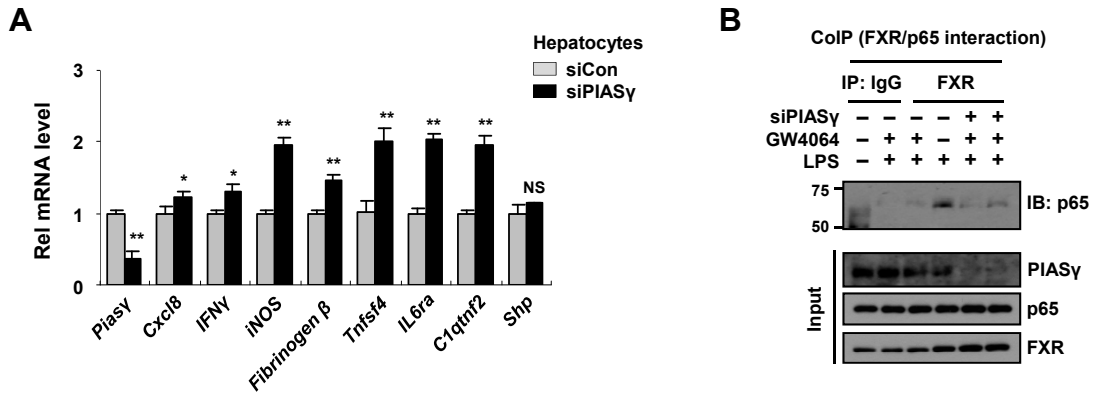


**Figure S10. Effects of downregulation of PIASy on inflammatory gene expression and FXR interaction with the p65 subunit of NF-κB in hepatocytes.**

(A) Hepatocytes were isolated from lean mice and transfected with control siRNA or siRNA for PIASy, and mRNA levels of indicated genes were detected by q-RTRPCR. (n=3, *p<0.05, **p<0.005, NS, not significant). (B) Primary mouse hepatocytes were transfected with control siRNA or PIASy siRNA were infected with an adenoviral vector expressing FXR-WT, and then, treated with GW4064 and LPS as indicated. The p65 subunit of NF-κB was detected by CoIP.

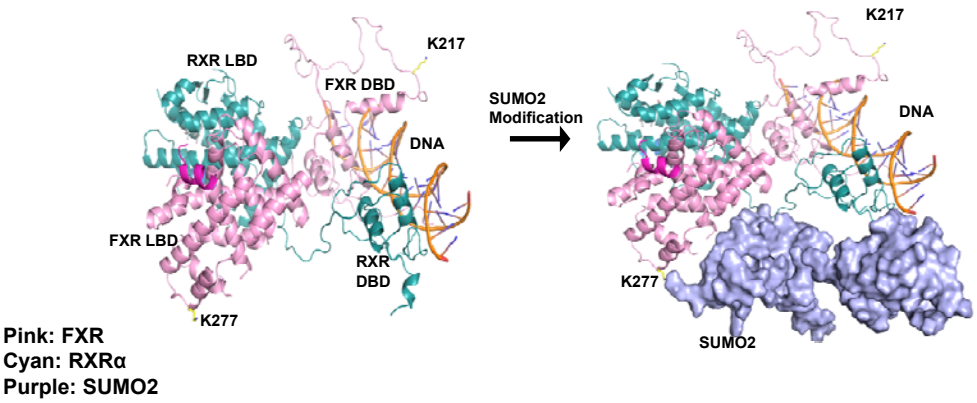


**Figure S11. Structural modeling analysis: Effects of SUMO2 modification of FXR on interaction with RXRα on DNA.**
The predicted structure of FXR and RXR bound to DNA based on the RXRa/LXRβ/DNA (4NQA) structure with the LXRβ replaced by FXR (3BEJ) is shown. The positions of K217 and K277 in FXR are indicated. K277 in the LBD of FXR is located in the interface with the RXR DBD (left). SUMO2 modification (dimmers of SUMO2 are shown) of the LBD of FXR would block the interaction of FXR with RXRα (right).

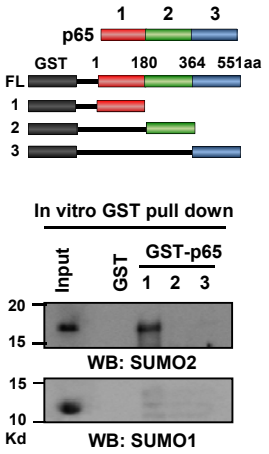


**Figure S12. The p65 subunit of NF-κB directly interacts with SUMO2, but not with SUMO1.**
A schematic of the domains of p65 that were fused to GST is shown at the top. The interaction between SUMO1/2 and p65 domains was detected by GST-pull down followed by IB.

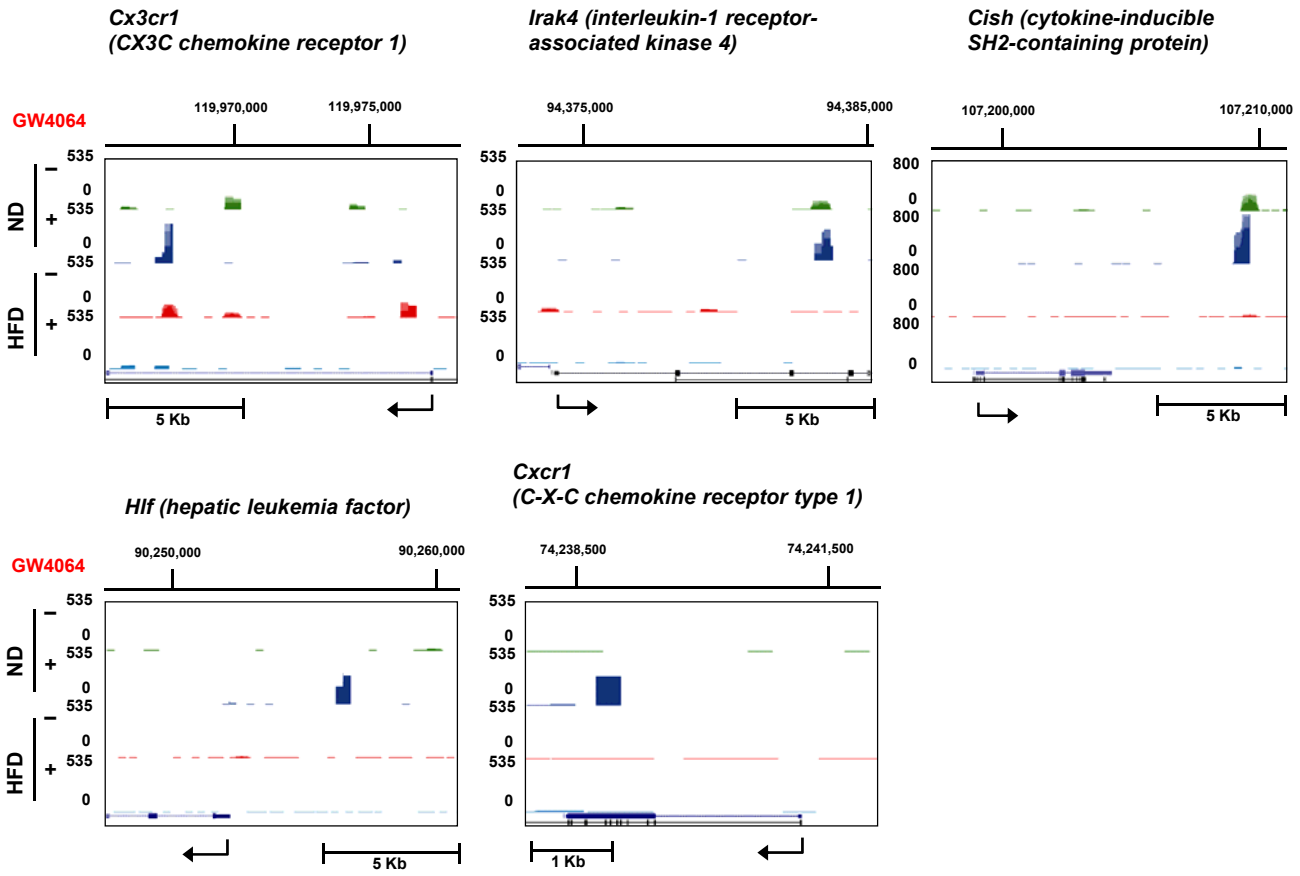


**Figure S13. Effects of GW4064 treatment on hepatic FXR binding sites near inflammatory genes in mice fed ND or HFD** .

USSC browser plots of FXR hepatic binding peaks from our published ChIP-seq studies (Lee et al. Hepatology, 2012). Results are shown for mice fed either a ND or HFD and treated i.p. with vehicle (-) or GW4064 (+) for 1 h.

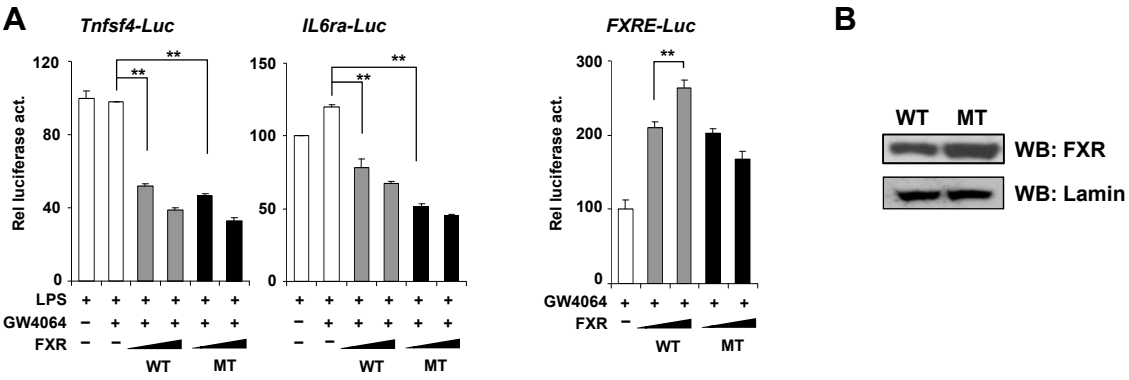


**Figure S14. Cell-based luciferase reporter assay:**
**Effects of mutation of the FXR DNA binding domain (DBD) on the activity of luciferase driven by either inflammatory genes or FXR/RXR target genes.**
(A) Luciferase reporters containing with the NF-κB binding site in *Tnfsf4* or *IL6ra* or an FXRE were constructed. HepG2 cells were transfected with the reporter vector and either FXR WT or the DBD mutant lacking DNA binding (MT) in mutation at the first zinc finger as indicated and treated with GW4064 and LPS. Luciferase activities were measured (n=3, **p<0.005, NS, not significant). (B) Expression levels of the FXR WT and mutant were detected by IB with lamin as a loading control.

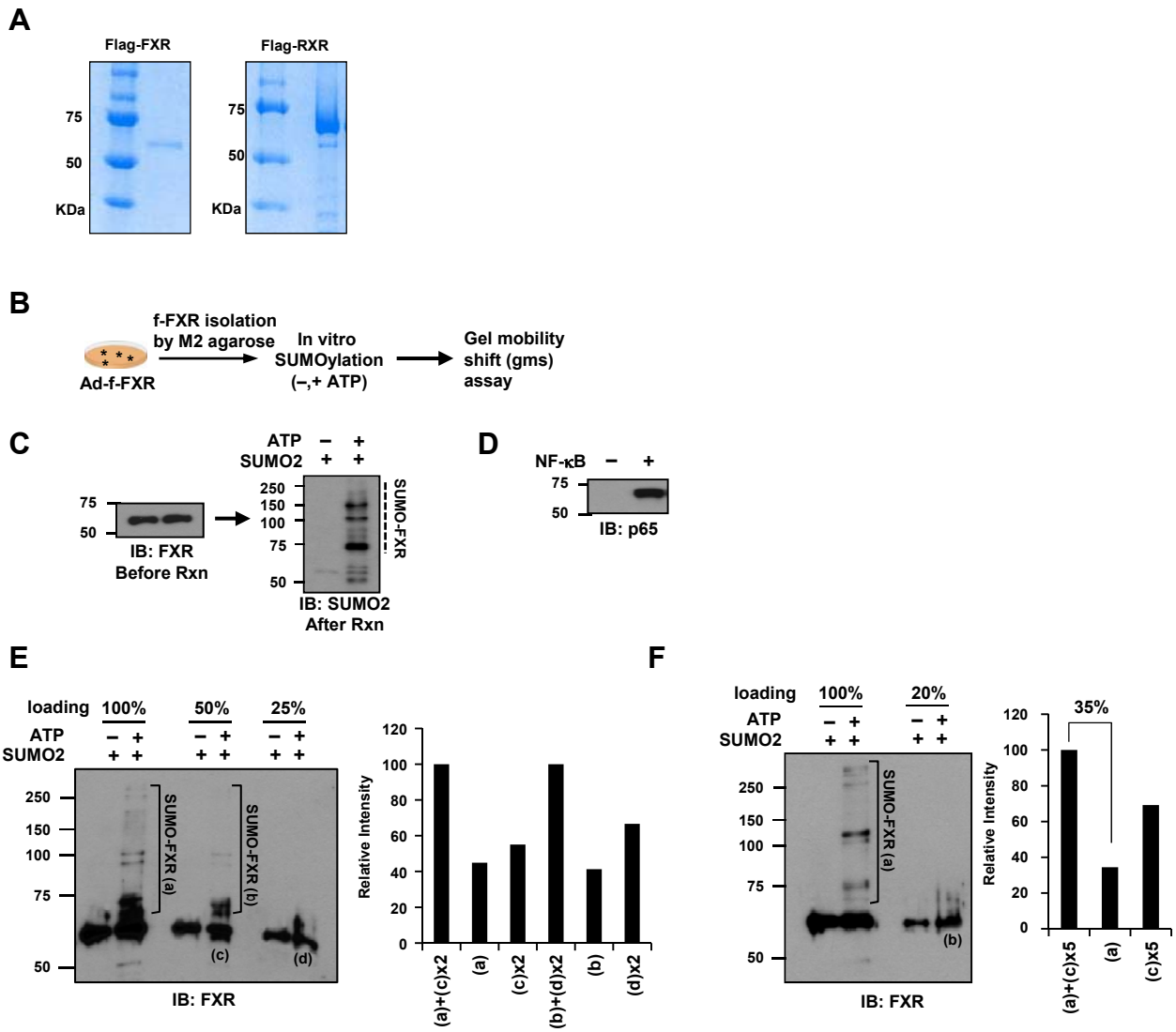


**Figure S15. Analysis of proteins used for gel-shift assays.**
(A) Flag-FXR and flag-RXR were expressed in bacteria, isolated by M2 agarose, and partially purified proteins were visualized by colloidal staining. (B) Experimental outline for gel mobility shift (gms) assay. (C) Flag-FXR-WT was incubated with purified SUMO components with (+) and without (-) ATP as described in Methods and Materials. Input amounts in the two reactions are shown (left) and SUMO2 modification of FXR detected by IB is shown at the right. (D) Cos-1 cells were transfected with expression plasmids for p65 and p50, and 48 h later, cell were treated with LPS for 15 min and nuclear extracts were prepared. Expression of p65 were detected by IB. (E, F) Fraction of FXR SUMOylated in in vitro SUMO assays. Purified flag-FXR WT was incubated with SUMO components with and without ATP as indicated. Varying amounts of the samples were analyzed by gel electrophoresis and FXR was detected by IB with antibody to FXR. (E) 25% and 50% of the initial amount (100%) were analyzed and (F) 20% of the initial amount (100%) was analyzed. The intensity of the bands for FXR and SUMO-FXR were analyzed using Image J and plotted with the total (FXR + SUMO-FXR) set as 100. The percentage of SUMO-FXR as indicated in the figure ranged from 35%-44% in these experiments.

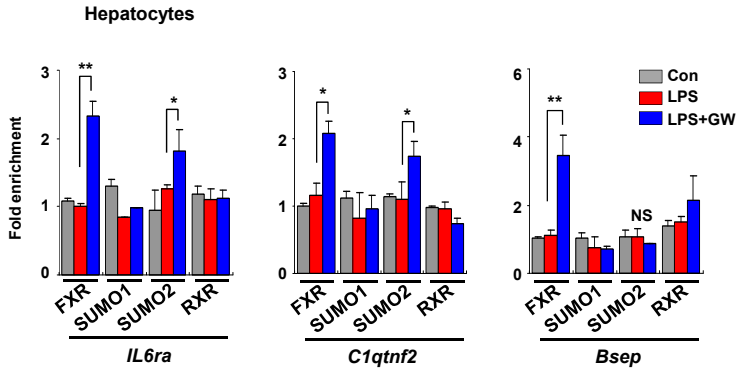


**Figure S16. Effects of treatment with GW4064 and LPS on occupancy of endogenous FXR, SUMO1, SUMO2 and RXR at inflammatory and FXR/RXR target genes.**

Hepatocytes from WT mice were treated with LPS and/or GW4064 as indicated and ChIP assays were performed using antibodies to FXR, SUMO1, SUMO2 or RXR. Three independent hepatocyte isolation followed by ChIP assays were performed. Sequences of the indicated genes in the immunoprecipitates were detected by q-PCR (n=3, *p<0.05, **p<0.005)

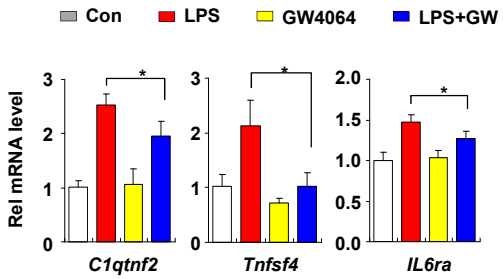


**Figure S17. Effects of GW4064 and/or LPS treatment on expression of direct FXR target inflammatory genes.**
Hepatocytes were isolated from mice, treated with LPS and/or GW4064 as indicated, and mRNA levels of direct FXR target inflammatory genes were measured (SEM, n=3, *p<0.05).

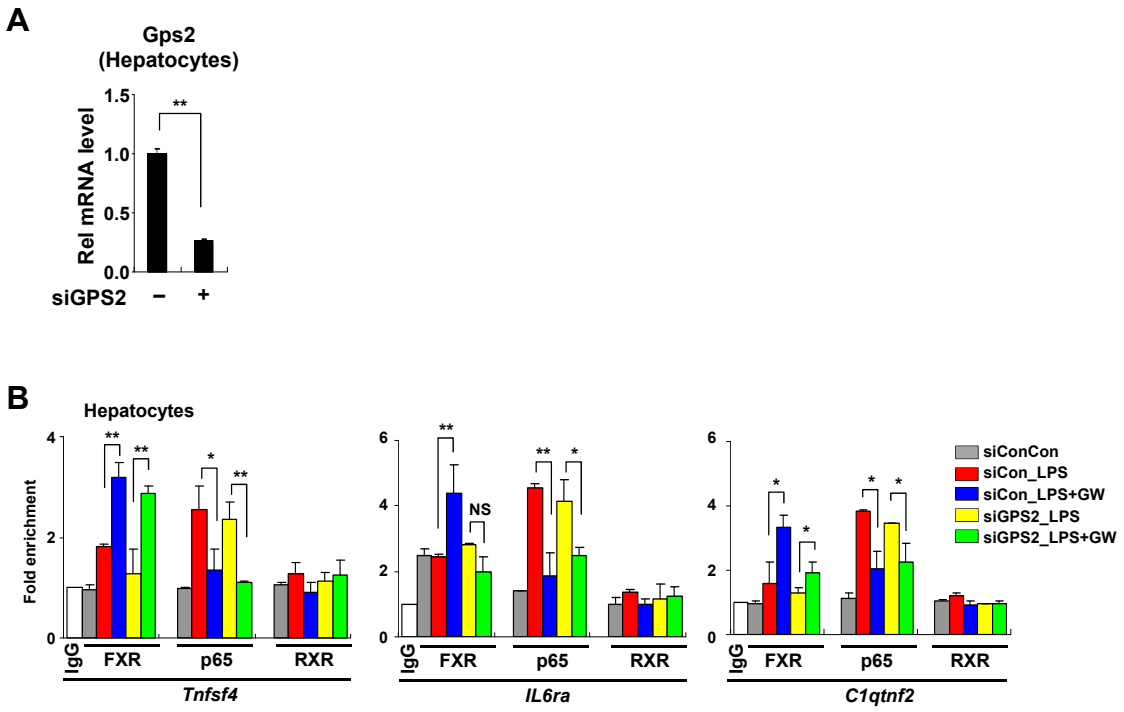


**Figure S18. Effects of downregulation of GPS2 on occupancy of FXR, RXR, and p65 at inflammatory genes.**

(A) The mRNA levels of GPS2 after downregulation by GPS2 siRNA were detected by q-RTPCR. (B) ChIP: Hepatocytes from WT mice were transfected with control siRNA (siCon) or GPS2 siRNA (siGPS2) and then, treated with GW4064 and LPS as indicated. Three independent assays were performed. Occupancy of endogenous FXR, p65 and RXR was detected by q-PCR (n=3, *p<0.05, **p<0.005).

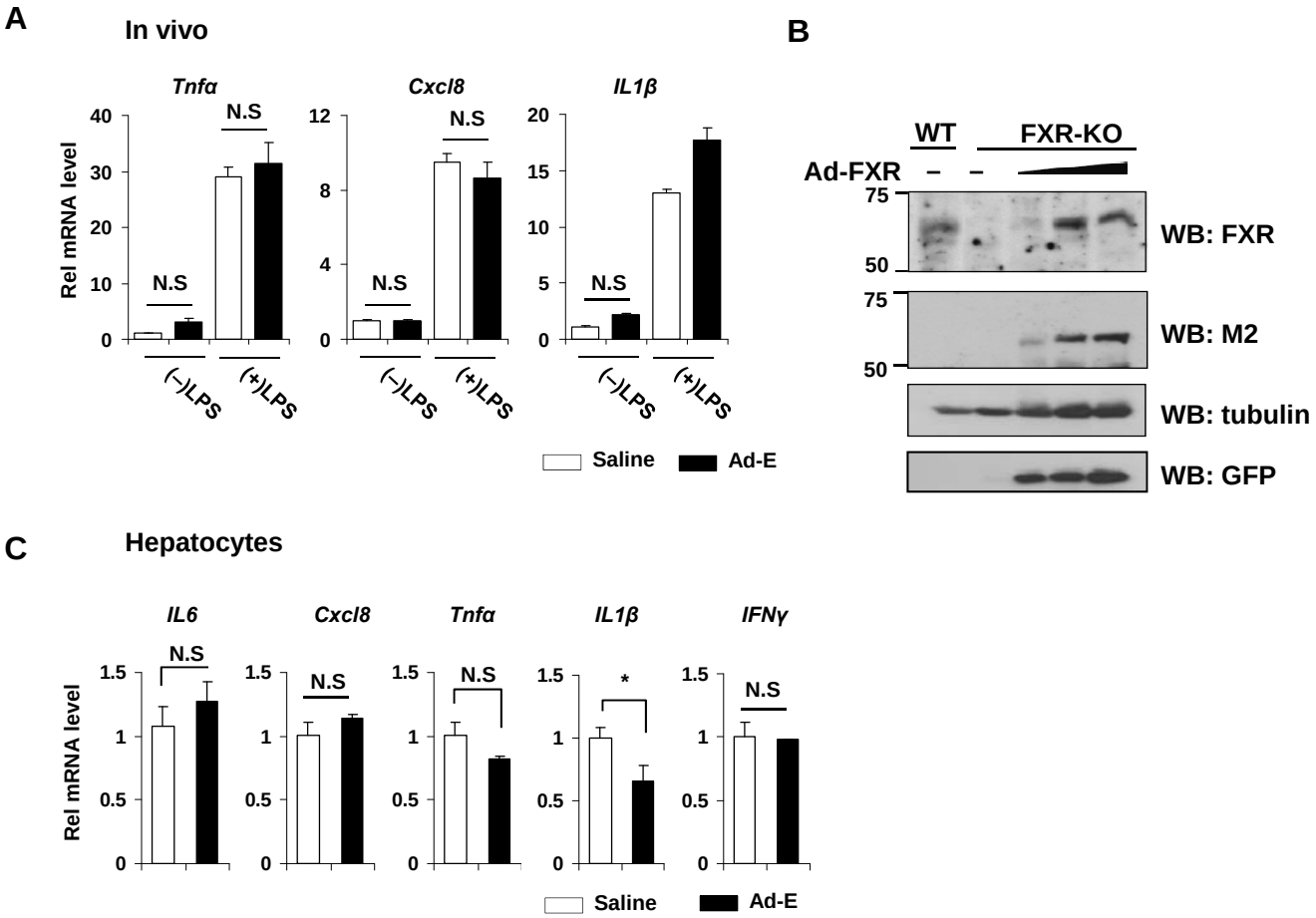


**Fig. S19. Control experiments for adenoviral-mediated expression of FXR in WT and FXR-KO mice.**

(A) Effects of adenoviral infection on inflammatory gene expression: To examine whether inflammatory genes are induced at the viral dose used, mice were injected via the tail vein with Ad-empty (2.5 X $10^8$ pfu/100 μl saline) or vehicle saline and 7 days later, mice were treated with LPS or vehicle for 6 h and livers were collected for q-RTPCR to measure mRNA levels of inflammatory genes (n=4, NS statistically not significant).
(B) Levels of adenovirally expressed exogenous FXR in FXR-KO hepatocytes are similar to endogenous FXR levels in WT mouse hepatocytes: Hepatocytes were prepared from WT mice or FXR-KO mice and infected with increasing adenoviral doses (Ad-flag-FXR) as indicated and protein levels of FXR, flag-FXR, tubulin, and GFP were detected by IB.
(C) Effects of adenoviral infection on inflammatory gene expression in hepatocytes: Hepatocytes were infected with Ad-empty (2.5 X $10^8$ pfu/100 μl saline) or vehicle saline and 2-3 days later, mRNA levels of inflammatory genes were measured by q-RTPCR. (n=3, *p<0.05, NS statistically not significant).

## Table S1. Microarray data of FXR K217Q mutant vs WT in normal diet mice.

| ID | Gene Name | Species |
|---|---|---|
| **Down_ND_K217Q vs WT** | | |
| ILMN_1213286 | chemokine (C-C motif) ligand 21A; predicted gene 1987 | Mus musculus |
| ILMN_1215209 | C-type lectin domain family 4, member e | Mus musculus |
| ILMN_1215862 | chemokine (C-X-C motif) ligand 9 | Mus musculus |
| ILMN_1218525 | interleukin 18 receptor 1 | Mus musculus |
| ILMN_1245710 | chemokine (C-C motif) ligand 2 | Mus musculus |
| ILMN_1246073 | left right determination factor 1 | Mus musculus |
| ILMN_2424299 | tumor necrosis factor receptor superfamily, member 12a | Mus musculus |
| ILMN_2473562 | linker for activation of T cells family, member 2 | Mus musculus |
| ILMN_2591361 | CD28 antigen; similar to CD28 antigen | Mus musculus |
| ILMN_2682566 | interleukin 1 receptor antagonist | Mus musculus |
| ILMN_2705628 | C-type lectin domain family 4, member d | Mus musculus |
| ILMN_2733793 | coronin, actin binding protein 1A | Mus musculus |
| ILMN_2760800 | chemokine (C-X-C motif) ligand 14 | Mus musculus |
| ILMN_2771766 | chemokine (C-C motif) ligand 12; similar to monocyte chemoattractant protein-5 | Mus musculus |
| ILMN_2777498 | interleukin 1 beta | Mus musculus |
| ILMN_2778289 | chemokine (C-X-C motif) ligand 2 | Mus musculus |
| ILMN_2804685 | defensin beta 1 | Mus musculus |
| ILMN_2835117, ILMN_2771176 | chemokine (C-C motif) ligand 7 | Mus musculus |
| ILMN_2835423 | complement factor D (adipsin) | Mus musculus |
| ILMN_2836386 | chemokine (C-C motif) ligand 19 | Mus musculus |
| ILMN_2867076 | histocompatibility 2, O region alpha locus | Mus musculus |
| ILMN_2948552 | chemokine (C motif) ligand 1 | Mus musculus |
| ILMN_2969845, ILMN_2640848, ILMN_2602139 | predicted gene 13304; similar to beta chemokine Exodus-2 | Mus musculus |
| ILMN_3122961 | guanylate binding protein 2 | Mus musculus |
| **Down_ND_K217Q vs WT** | | |
| ILMN_1213632 | phosphoenolpyruvate carboxykinase 1, cytosolic | Mus musculus |
| ILMN_1225718 | 3-hydroxy-3-methylglutaryl-Coenzyme A reductase | Mus musculus |
| ILMN_1227596 | phosphomevalonate kinase | Mus musculus |
| ILMN_1228752 | myo-inositol 1-phosphate synthase A1 | Mus musculus |
| ILMN_1229529 | hydroxysteroid (17-beta) dehydrogenase 7 | Mus musculus |
| ILMN_1233469 | low density lipoprotein receptor | Mus musculus |
| ILMN_1234449 | hydroxy-delta-5-steroid dehydrogenase, 3 beta- and steroid delta-isomerase 5 | Mus musculus |
| ILMN_1239239 | prostaglandin-endoperoxide synthase 1 | Mus musculus |
| ILMN_1239601 | mevalonate kinase; similar to mevalonate kinase | Mus musculus |
| ILMN_1242564 | RIKEN cDNA C730007P19 gene; similar to androgen-repressible liver protein SMP-2 | Mus musculus |
| ILMN_1250008 | choline kinase alpha | Mus musculus |
| ILMN_1253008 | acetyl-Coenzyme A acetyltransferase 2 | Mus musculus |
| ILMN_1253224, ILMN_2752940, ILMN_2620106 | 24-dehydrocholesterol reductase | Mus musculus |
| ILMN_2540103, ILMN_1225730 | similar to farnesyl diphosphate synthetase; farnesyl diphosphate synthetase | Mus musculus |
| ILMN_2590923 | similar to Isopentenyl-diphosphate delta isomerase | Mus musculus |
| ILMN_2613908 | arachidonate 12-lipoxygenase | Mus musculus |
| ILMN_2614161 | lanosterol synthase | Mus musculus |
| ILMN_2614752 | predicted gene 11295; ELOVL family member 6 | Mus musculus |
| ILMN_2645275 | mevalonate (diphospho) decarboxylase | Mus musculus |
| ILMN_2654952 | similar to Hmgcs1 protein; 3-hydroxy-3-methylglutaryl-Coenzyme A synthase 1 | Mus musculus |
| ILMN_2660471 | 7-dehydrocholesterol reductase | Mus musculus |
| ILMN_2683113 | angiogenin, ribonuclease, RNase A family, 5 | Mus musculus |
| ILMN_2688075 | cytochrome P450, family 51 | Mus musculus |
| ILMN_2720479 | lysophosphatidylglycerol acyltransferase 1 | Mus musculus |
| ILMN_2725402, ILMN_2958207, ILMN_2594525, ILMN_2594521 | NAD(P) dependent steroid dehydrogenase-like | Mus musculus |
| ILMN_2726412 | estrogen receptor 1 (alpha) | Mus musculus |
| ILMN_2752782 | aldo-keto reductase family 1, member D1 | Mus musculus |
| ILMN_2756023 | proprotein convertase subtilisin/kexin type 9 | Mus musculus |
| ILMN_2777462 | patatin-like phospholipase domain containing 3 | Mus musculus |
| ILMN_2823778 | sterol-C4-methyl oxidase-like | Mus musculus |
| ILMN_2826869 | serum amyloid A 1 | Mus musculus |
| ILMN_2858121, ILMN_2709810 | acyl-coenzyme A amino acid N-acyltransferase 2 | Mus musculus |
| ILMN_2874352 | cytochrome P450, family 17, subfamily a, polypeptide 1 | Mus musculus |

## Table S2. Microarray data of FXR K217R vs WT in high fat diet mice.

| ID | Gene Name | Species |
|---|---|---|
| **Up_HFD_K217R vs WT** | | |
| ILMN_1214531 | cytochrome P450, family 2, subfamily b, polypeptide 13 | Mus musculus |
| ILMN_1229267, ILMN_1244847, ILMN_2734598, ILMN_3159131, ILMN_3079804 | cytochrome P450, family 2, subfamily a, polypeptide 21 | Mus musculus |
| ILMN_1234449 | hydroxy-delta-5-steroid dehydrogenase, 3 beta- and steroid delta-isomerase 5 | Mus musculus |
| ILMN_1243516 | fat storage-inducing transmembrane protein 1 | Mus musculus |
| ILMN_1246069 | NADH dehydrogenase (ubiquinone) 1, alpha/beta subcomplex, 1 | Mus musculus |
| ILMN_1246446 | leucine rich repeat containing 59 | Mus musculus |
| ILMN_1247832 | CD74 antigen | Mus musculus |
| ILMN_1250364 | cytochrome P450, family 2, subfamily a, polypeptide 4 | Mus musculus |
| ILMN_2433685 | ectonucleoside triphosphate diphosphohydrolase 5 | Mus musculus |
| ILMN_2604383 | cytochrome P450, family 7, subfamily a, polypeptide 1 | Mus musculus |
| ILMN_2617625 | cytochrome P450, family 2, subfamily b, polypeptide 9 | Mus musculus |
| ILMN_2627744 | cytochrome P450, family 8, subfamily b, polypeptide 1 | Mus musculus |
| ILMN_2641678 | 3-hydroxybutyrate dehydrogenase, type 2 | Mus musculus |
| ILMN_2644350 | thymus cell antigen 1, theta | Mus musculus |
| ILMN_2647234, ILMN_2772070 | deiodinase, iodothyronine, type I; similar to Dio1 protein | Mus musculus |
| ILMN_2666018 | matrix Gla protein | Mus musculus |
| ILMN_2680827 | interleukin 7 receptor | Mus musculus |
| ILMN_2691295 | cytochrome P450, family 26, subfamily a, polypeptide 1 | Mus musculus |
| ILMN_2697415 | CD3 antigen, delta polypeptide | Mus musculus |
| ILMN_2730425, ILMN_2733073 | ryanodine receptor 1, skeletal muscle | Mus musculus |
| ILMN_2736539 | cytochrome P450, family 2, subfamily c, polypeptide 55 | Mus musculus |
| ILMN_2739847, ILMN_2795106 | cytochrome P450, family 1, subfamily a, polypeptide 2 | Mus musculus |
| ILMN_2750035 | neurexin I | Mus musculus |
| ILMN_2753697 | CD2 antigen | Mus musculus |
| ILMN_2827217 | calsyntenin 3 | Mus musculus |
| ILMN_2830666 | RIKEN cDNA 9130409I23 gene | Mus musculus |
| ILMN_2841328 | Vac14 homolog (S. cerevisiae) | Mus musculus |
| ILMN_2850342 | cytochrome b-561 domain containing 2 | Mus musculus |
| ILMN_2875737 | cytochrome P450, family 2, subfamily d, polypeptide 12 | Mus musculus |
| ILMN_2896768 | carbonyl reductase 3 | Mus musculus |
| ILMN_2917386 | glutathione S-transferase | Mus musculus |
| **Down_HFD_K217R vs WT** | | |
| ILMN_1218075 | fibrinogen beta chain | Mus musculus |
| ILMN_1221700 | elastase 2, neutrophil | Mus musculus |
| ILMN_1223880 | transmembrane protease, serine 2 | Mus musculus |
| ILMN_1225218 | kininogen 1 | Mus musculus |
| ILMN_1228474 | cathepsin J | Mus musculus |
| ILMN_1228718 | syndecan 1 | Mus musculus |
| ILMN_1228832 | neutrophilic granule protein | Mus musculus |
| ILMN_1228958 | follistatin | Mus musculus |
| ILMN_1237485, ILMN_2479977 | energy homeostasis associated | Mus musculus |
| ILMN_1253755, ILMN_1242370, ILMN_2897167 | fibrinogen-like protein 1 | Mus musculus |
| ILMN_1257574 | endothelial cell-specific molecule 1 | Mus musculus |
| ILMN_2524865 | chitinase 3-like 4 | Mus musculus |
| ILMN_2531773, ILMN_2984219 | cDNA sequence BC048546 | Mus musculus |
| ILMN_2543198 | nonagouti | Mus musculus |
| ILMN_2588227 | fibronectin 1 | Mus musculus |
| ILMN_2589915 | hyaluronan and proteoglycan link protein 4 | Mus musculus |
| ILMN_2600421, ILMN_2925094, ILMN_1249030 | myeloperoxidase | Mus musculus |
| ILMN_2617005, ILMN_2868699 | prolactin receptor | Mus musculus |
| ILMN_2659426 | chemokine (C-X-C motif) ligand 14 | Mus musculus |
| ILMN_2660969 | mannan-binding lectin serine peptidase 1 | Mus musculus |
| ILMN_2682613 | insulin-like growth factor binding protein 5 | Mus musculus |
| ILMN_2683113 | angiogenin, ribonuclease, RNase A family, 5 | Mus musculus |
| ILMN_2690603 | secreted phosphoprotein 1 | Mus musculus |
| ILMN_2692316 | dipeptidase 2 | Mus musculus |
| ILMN_2695360 | lipocalin 13 | Mus musculus |
| ILMN_2754364 | lactotransferrin | Mus musculus |
| ILMN_2757966 | platelet factor 4 | Mus musculus |
| ILMN_2758029 | proteinase 3 | Mus musculus |
| ILMN_2758571 | serum amyloid A 2 | Mus musculus |
| ILMN_2766604 | cathelicidin antimicrobial peptide | Mus musculus |
| ILMN_2771237 | lipopolysaccharide binding protein | Mus musculus |
| ILMN_2777087 | melanoma inhibitory activity 1 | Mus musculus |
| ILMN_2789900 | CD177 antigen | Mus musculus |
| ILMN_2803674 | S100 calcium binding protein A9 (calgranulin B) | Mus musculus |
| ILMN_2804685 | defensin beta 1 | Mus musculus |
| ILMN_2826869 | serum amyloid A 1 | Mus musculus |
| ILMN_2896170 | serum amyloid P-component | Mus musculus |
| ILMN_2930680 | leucine rich repeat and fibronectin type III domain containing 3 | Mus musculus |
| ILMN_2964560 | CD163 antigen | Mus musculus |
| ILMN_3008361 | BMP-binding endothelial regulator | Mus musculus |
| ILMN_3009880, ILMN_2653328 | interleukin 28 receptor alpha | Mus musculus |
| ILMN_3040693 | laminin gamma 3 | Mus musculus |

**Table S3. Lists of primer sequence.**

| No. | Gene | Forward (5'-3') | Reverse (5'-3') |
|---|---|---|---|
| **primer sequence for q-PCR** | | | |
| 1 | Bip | TCATCGGACGCACTTGGAA | CAACCACCTTGAATGGCAAGA |
| 2 | Bseb | GTCGGACCTGCATTGTCATTG | ATGTGTGTCTGAGATTCTTGCATT |
| 3 | Calreticulin | TTACGCACTGTCCGCCAAA | GCTCATGCTTCACCGTGAACT |
| 4 | Ccl2 | CCCAATGAGTAGGCTGGAGA | TCTGGACCCATTCCTTCTTG |
| 5 | Ccl7 | GTGTCCCTGGGAAGCTGTTA | ATAGCCTCCTCGACCCACTT |
| 6 | Chop | GTCCCTAGCTTGGCTGACAGA | TGGAGAGCGAGGGCTTTG |
| 7 | Coronin 1a | TCTGATCTGTGAGGCCAGTG | ATGTCTAGCACAGGGGCAGT |
| 8 | CRP | TATGGGAGAATGGTCGGAAC | TCAAGGGTCATCTGGTCCTC |
| 9 | Cxcl14 | TATCGTCACCACCAAGAGCA | CTTCTCGTTCCAGGCATTGT |
| 10 | Cxcl2 | TCCAGAGCTTGAGTGTGACG | TTCAGGGTCAAGGCAAACTT |
| 11 | Cxcl8(IL8) | TCACCGATGTCTACCTGCTG | CACAGGGTTGAGCCAAAAGT |
| 12 | F4/80 | TTACGATGGAATTCTCCTTGTATATCA | CACAGCAGGAAGGTGGCTATG |
| 13 | Fibrinogen-β | GTATTTGCTGGCCTCGTTCT | GGGACCCACAGAACTTCTCA |
| 14 | IFNγ | TGCTGATGGGAGGAGATGTCT | TTTCTTTCAGGGACAGCCTGTT |
| 15 | IL18ra | CCGATCACAAATTCATGTGG | GGTGGCTGTTTCATTCCTGT |
| 16 | IL1β | AACCTGCTGGTGTGTGACGTTC | CAGCACGAGGCTTTTTTGTTGT |
| 17 | IL6 | AGAAGGAGTGGCTAAGGACCAA | AACGCACTAGGTTTGCCGAGTA |
| 18 | iNOS | GATGGTCCGCAAGAGAGTGC | AACGTAGACCTTGGGTTTGCC |
| 19 | Mcad | GATCGCAATGGGTGCTTTTGATAGAA | AGTTGATTGGCAATGTCTCCAGCAAA |
| 20 | Mmp13 | ATCCTGGCCACCTTCTTCTT | TTTCTCGGAGCCTGTCAACT |
| 21 | p300 | GAGAAACTAGGCCTTGGCTTAGATG | GCGGCGGGAGTCTCCT |
| 22 | Saa1/2 | GTAATTGGGGTCTTTGCC | TTCTGCTCCCTGCTCCTG |
| 23 | Scara3 | TAAATCCGTCTCCCTCATGC | GGAGAGGTTTCGGACATTGA |
| 24 | Shp | CAAGAAGATTCTGCTGGAGG | GGATGTCAACATCTCCAATG |
| 25 | Sirt1 | CCTCCTGTTGACCGATGGAC | CTGGCGTGTGACGTTCTGTC |
| 26 | Tnfα | AGCCCCCAGTCTGTATCCTT | GGTCACTGTCCCAGCATCTT |
| 27 | C1qtnf2 | AAGGGACCTAAGGGCAAAAA | TGGGTAGCTCTTGGTTACCG |
| 28 | IL6ra | CCAGGTGCCCTGTCAGTATT | CTGGACTTGCTTCCCACACT |
| 29 | Tnfsf4 | CTGAACGATGGTCGAAGGAT | ACAACAATCAGCTCCCCATC |
| 30 | Sumo1 | ATTGGACAGGATAGCAGTGAGA | TCCCAGTTCTTTCGGAGTATGA |
| 31 | Sumo2 | GGACAGGATGGTTCTGTGGT | CGGAATCTGATCTGCCTCAT |
| 32 | Piasy | GCCTGGTGTGGAACCTAAGA | ATAGTTGCCCCAGGTGACAG |
| 33 | Fas | CCTGGATAGCATTCCGAACCT | AGCACATCTCGAAGGCTACACA |
| 34 | Gps2 | ATCGCCCAGGTACTCTGATG | AGCTGCTGATCCCACGTAGT |
| 35 | Srebp1c | GCTGTTGGCATCCTGCTATC | TAGCTGGAAGTGACGGTGGT |
| 36 | Acc1 | CGAAACTCCCAGAACTGCTC | TGCAATCTTATCCCCCAAAG |
| 37 | Scd1 | CCCAGTCGTACACGTCATTTT | CATCATTCTCATGGTCCTGCT |
| **primer sequence for ChIP-PCR and EMSA** | | | |
| 1 | C1qtnf2 | TCTAAGGAGCATGCCATGTG | GAGGGCGTGGTACCAAATAG |
| 2 | IL6ra | GGTACCCACAGATCCCAGAA | GTTGCTGAGGACCAAGTTGC |
| 3 | Tnfsf4 | AAATTTTGGTGCATGTGTGTG | GCCAAGCCTGATAACCTGAG |
| 4 | Shp | CAGTGAGAACCCTGGTCTT | CTGGCCAAACAACCTTGAC |
| 5 | Bsep | CGACCTTTCCTCTCATGTCA | CATTGAACAGAAATCAGGCTTTT |
| 6 | Shp (EMSA) | TGGTACAGCCTGAGTTAATGACCTTGTTTATC | GATAAACAAGGTCATTAACTCAGGCTGTACCA |
| 7 | Tnfsf4 (EMSA) | CCTGATCAAGGCTAAAGAAAAGCCAGTACTAA | TTAGTACTGGCTTTTCTTTAGCCTTGATCAGG |